Resonant Electron Capture and Stripping in Ne^+-Ne Collisions at Energies of Several keV*

P. R. JONES, P. COSTIGAN, AND G. VAN DYK
Hasbrouck Physics Laboratory, University of Massachusetts, Amherst, Massachusetts
(Received 2 August 1962)

Measurements have been made for collisions in which Ne^+ ions are incident upon neutral Ne atoms. The incident ions ranged in energy from 0.80 to 15 keV and were scattered through angles of from 3° to 13° in the laboratory coordinates. The target atoms were present in the form of a gas at a pressure sufficiently low to insure that the bulk of the scattered particles reaching the detectors had experienced only a single encounter with a target atom. Analysis of the scattered incident particles shows that the relative probabilities for electron capture, scattering without change of charge, and single electron stripping all oscillate rapidly as a function of scattering angle. This behavior is evidently the result of resonance of the Ne^+-Ne system between the attractive and repulsive states characteristic of the homonuclear, diatomic molecular ion. The data are discussed in terms of this interpretation, and experimental values are presented for the energy difference (E_r-E_a) integrated over the collision path of relative motion, E_r and E_a being the energies of the repulsive and attractive states, respectively. For the range of collisions studied, this integrated energy difference ranged from about 15 eV-Å to about 120 eV-Å. An approximate functional dependence of (E_r-E_a) upon internuclear separation is obtained from the data.

1. INTRODUCTION

THE present experimental study is concerned with the charge-changing features of single collisions of Ne^+ with Ne, the charge analysis of the scattered particles being carried out at each of several angles of scattering and the entire angular survey being repeated at each of several energies of incident ion. For these collisions the angular distribution of the scattered incident particles is heavily weighted in the forward direction, with a corresponding tendency for the recoil particles to be scattered at large angles to the direction of the incident ions. Thus, the particles emerging at the relatively small angles selected in this study are predominantly the scattered incident particles.

Similar experiments[1,2] with the noble gases have been performed at incident-ion energies of 25 keV and above, but the more recent measurements of Ziemba *et al.*[3] show a particularly interesting effect in collisions of Ar^+ on Ar and Ne^+ on Ne at energies below about 25 keV; the probability of electron capture by the incident ion at a particular energy is found to oscillate as a function of the angle through which the incident particle is scattered. In particular, the electron capture probability in collisions of Ne^+ on Ne is seen to have three local maxima in the angular range of 3° to 10° for both 10 and 15 keV incident-ion energy.

A small part of the present work duplicates the above measurements of Ziemba, and the agreement is found to be good. An interpretation of the data is given in terms of the description of resonant electron capture provided by Holstein,[4] in which the electron moves back and forth between the two atoms during the course of the collision. A still more quantitative picture of the collision process is obtained by using the scattering calculation of Everhart *et al.*[5] and the potential energy functions of Lane and Everhart[6] to relate the observed energy and scattering angle to the distance of closest approach for the collision.

The data of this paper are in many ways quite similar to the data of Lockwood and Everhart,[7] who performed an experiment in which protons were incident upon neutral hydrogen atoms. Furthermore, the interpretation they give to the observed behavior of the electron capture probability is consistent with that given in this paper by application of Holstein's results. Other theoretical treatments of resonant electron capture in ion-atom collisions are given by Bates and co-workers,[8,9] by Ziemba and Russek,[10] and by Bates[11] in a recent book.

2. DESCRIPTION OF THE APPARATUS

The Ne^+ ions were furnished by the Hasbrouck positive-ion accelerator which was constructed especially for this, and related, studies. The accelerator supplies to the collision chamber a focused, collimated beam of monoenergetic, magnetically analyzed positive ions, variable in energy from about 500 eV to 25 keV.

The positive ions are formed by rf excitation of the source gas (neon in this case) in an Oak Ridge type ion source. Upon being ejected from the source the positive ions are accelerated and focused in several stages by axially symmetric electrostatic fields. The ion beam is then deflected through 15° by an analyzing magnet and

* This work was supported by a grant from the National Science Foundation.
[1] E. N. Fuls, P. R. Jones, F. P. Ziemba, and E. Everhart, Phys. Rev. **107**, 704 (1957).
[2] P. R. Jones, F. P. Ziemba, H. A. Moses, and E. Everhart, Phys. Rev. **113**, 182 (1959).
[3] F. P. Ziemba, G. J. Lockwood, G. H. Morgan, and E. Everhart, Phys. Rev. **118**, 1552 (1960).
[4] T. Holstein, J. Phys. Chem. **56**, 832 (1952).
[5] E. Everhart, G. Stone, and R. J. Carbone, Phys. Rev. **99**, 1287 (1955).
[6] G. H. Lane and E. Everhart, Phys. Rev. **120**, 2064 (1960).
[7] G. J. Lockwood and E. Everhart, Phys. Rev. **125**, 567 (1962).
[8] D. R. Bates, H. S. W. Massey, and A. L. Stewart, Proc. Roy. Soc. (London) **A216**, 437 (1953).
[9] D. R. Bates and R. McCarroll, Proc. Roy. Soc. (London) **A245**, 175 (1958).
[10] F. P. Ziemba and A. Russek, Phys. Rev. **115**, 922 (1959).
[11] D. R. Bates, *Quantum Theory* (Academic Press Inc., New York and London, 1961), Vol. I, pp. 290–292.

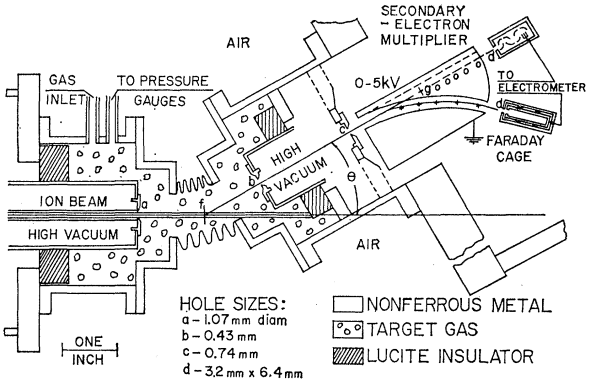

FIG. 1. The apparatus: collision chamber, electrostatic analyzer, and detectors.

passes between several sets of electrostatic deflection plates before arriving at the entrance to the collision chamber.

Figure 1 shows the collision chamber, the electrostatic analyzer, and the two detectors used in the measurements. The ion beam enters the collision chamber through hole a into a region of low-pressure target gas. A small fraction of these incident ions suffer collisions in the vicinity of the point f and of these a few are scattered through the appropriate angle θ allowing them to pass through holes b and c. These scattered particles then pass between the plates of the electrostatic analyzer where they can be separated according to their charge, providing for individual measurement of each component of the scattered beam. The proper positive voltage applied to the upper analyzer plate causes the doubly ionized ions, for instance, to follow the circular path shown, leaving the neutral atoms to proceed undeflected through a slot in the upper plate. In this case any singly ionized ions present in the scattered beam would follow some intermediate path (not shown in the figure), reaching neither detector.

The entire apparatus to the right of the flexible bellows can be rotated about an axis of rotation extending through the point f and perpendicular to the plane of the figure, allowing for the selection of any desired scattering angle θ. The Faraday cage and secondary-electron multiplier (SEM) both have a common mounting which can rotate inside the vacuum system about an axis through the point g. This latter rotation allows either detector to examine any charge component of the scattered beam.

Each of the tubes containing the holes a and b, respectively, can be seen to be insulated from ground and is provided with a lead wire to an outside galvanometer circuit which serves as a beam-monitoring device. For all angles θ somewhat less than that shown in Fig. 1 (including all angles for which data have thus far been taken) the entire unscattered portion of the incident ion beam falls upon the latter electrode. The observation of the current drawn by this electrode amounts to a monitoring of the ion beam inside the collision chamber and provides assurance that the incident ion beam has remained constant during the time that the various components of the scattered beam have been measured.

The SEM is a DuMont 6467 photomultiplier tube with the glass envelope and photocathode removed to allow the scattered particles to strike the first dynode directly. The first dynode is held at a negative voltage of about 2.0 kV, the anode being at approximately ground potential. The anode current is measured by a dc electrometer circuit, as is the current from the Faraday cage detector.

The target gas is supplied to the collision chamber from a one-liter Pyrex glass flask of Airco high-purity neon gas. The gas is metered through a variable leak and then passes through a liquid-nitrogen cold trap before entering the collision chamber. The target-gas pressure inside the collision chamber is controlled by adjusting the variable leak to give the appropriate flow of gas into the chamber. The gas flows out of the chamber through the holes a and b into the vacuum system, a 700 liter/sec oil diffusion pump maintaining a pressure of less than 10^{-6} Torr during typical operating conditions for the experiment.

3. METHOD OF MEASUREMENT

Each run was performed at a fixed energy of the incident ions, the data being obtained at each of several scattering angles. At a particular angle of scattering the scattered particle current in each charge state was measured by the detectors. The SEM was used for most of these measurements, since it has the dual advantage over the Faraday cage of being the more sensitive detector and being capable of detecting neutral particles. Once the gas-scattered currents had been measured, the target-gas supply to the collision chamber was shut off and the measurement repeated to determine the scattered currents due to residual gas. These currents were subtracted from the corresponding gas-scattered currents, this correction being typically about 10% but rising as high as 30% in a few cases. The fraction P_n of the scattered particles in each charge state was then determined from these corrected particle currents at each angle of scattering.

It was necessary to establish that the target-gas pressure was sufficiently low to insure that most of the scattered particles reaching the detectors were the result of a single interaction of an incident Ne^+ ion with a neutral Ne target atom. Consequently, at each of several energies and scattering angles the fractions P_n were measured as a function of target-gas pressure. It was observed that these fractions were independent of pressure for pressures less than some critical value of the order of one micron of mercury. The data presented in this paper were gathered for target-gas pressures somewhat less than this critical pressure.

In calculating the fraction P_n from the SEM readings it was necessary to take account of the fact that this detector has a sensitivity which varies with the charge on the incident particle. This arises from the fact that the first dynode is held at 2000 V negative with respect to ground, so that the kinetic energy of the particles striking this dynode during a given charge analysis varies by multiples of 2000 eV, depending upon the charge of the particles. Since the average number of emitted electrons per incident particle depends upon the kinetic energy of the incident particles, this resulted in the variation of sensitivity with charge, and the fractions P_n could not be calculated directly from the output currents of this detector. The determination of the sensitivity of the SEM for various charges on the incident particle was made in the following two ways:

(1) It was assumed that the sensitivity of this detector for neon atoms or ions is a function only of the kinetic energy with which the incident atoms or ions strike the first dynode, i.e., there is no explicit dependence of the sensitivity upon charge. (Evidence in support of this assumption is cited in the paper by Ziemba *et al.*,[3] who also used the DuMont 6467. Part of this evidence comes from previous work by one of the present authors.[2]) The sensitivity of this detector for Ne^+ was then determined for various kinetic energies of Ne^+ incident upon the first dynode by comparing the readings produced by this particle current on the SEM and the Faraday cage, respectively. These data then furnished a curve of SEM sensitivity *vs* kinetic energy which was used in the following way: The sensitivities for neutral, singly ionized, and doubly ionized particles all entering the SEM with the same kinetic energy E were taken from the curve to be the sensitivities at kinetic energies E, $E+2.0$ keV, and $E+4.0$ keV, respectively. A limitation on this method was imposed by the fact that the above curve could only be constructed in principle for energies above 2.0 keV, and in practice for energies above 2.5 keV, making unavailable the sensitivity for neutral particles at energies below 2.5 keV.

(2) The rapid oscillations with angle of the neutral fraction P_0, shown in Fig. 3, provided at the lower energies (where there are no doubly ionized particles present) a measure of the relative sensitivities for neutral and singly ionized particles. It is a well-established fact that the total (i.e., irrespective of charge on the particle) scattered particle current between the angles $(\theta-\Delta\theta)$ and $(\theta+\Delta\theta)$ for ion-atom collisions of the kind being studied here is a rather well-behaved monotonically decreasing function of the scattering angle θ, whose relative rate of decrease with angle is much less for the larger angles θ than for the smaller angles. It was observed, however, that when the total scattered particle current was being received by the SEM the output reading of this detector oscillated as a function of the scattering angle θ, reaching a maximum when P_0 was a minimum and a minimum when P_0 was a maximum. This apparent oscillation of the total scattered particle current with angle was quite evidently due to the relatively low sensitivity of the SEM for neutral particles, together with the rapid oscillation of P_0 with angle. It was thus possible to use these oscillations in the SEM readings of the total scattered particle current, together with the assumption that this latter current is actually a well-behaved monotonic function of scattering angle, to determine the relative sensitivities for neutral and singly ionized particles. Fortunately, it is at the lower energies where this effect is most pronounced, providing a measurement of relative sensitivities at those energies for which method (1) is not applicable.

Some of the data at the lower energies and larger angles of scattering were obtained by replacing the old DuMont 6467 SEM with a DuMont SP-182, the latter being the same as the 6467 except that the cesium and photocathode are omitted in the assembly. The dynode structure of the SP-182 was exposed to air for about 10 min between the time the glass envelope was removed and the start of pump down after installation in the apparatus. The gain of the SP-182 was found to be on the order of 10^5, almost 100 times that of the 6467, which had been exposed to air for extended periods on many occasions. Many spot checks were made at various energies and angles and the data were found to be reproducible with this new SEM.

4. DATA

The data are shown in Figs. 2–4. The left half of Fig. 2 is a plot of the fraction of the scattered particles which are singly ionized P_1 vs the scattering angle θ in laboratory coordinates at each of several energies of incident Ne^+. The right half of Fig. 2 is a similar plot

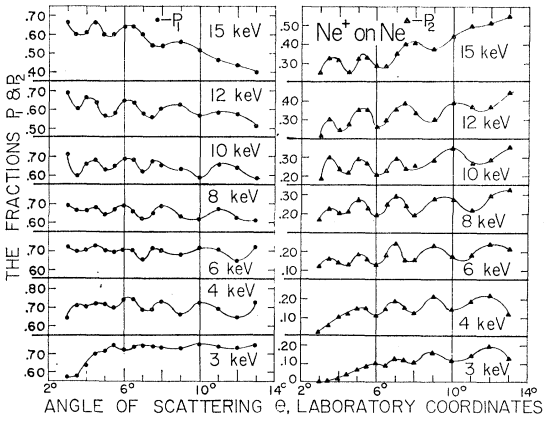

FIG. 2. The singly ionized fraction of the scattered incident particles P_1, and the doubly ionized fraction P_2, are shown vs scattering angle for each of several kinetic energies of the incident Ne^+ ion. Neutral Ne atoms are the targets, the target gas being at a sufficiently low pressure to insure the predominance of single collisions.

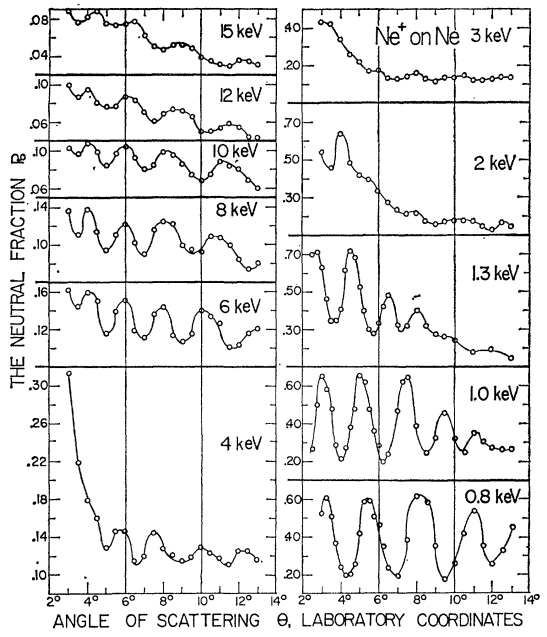

FIG. 3. The neutral fraction of the scattered incident particles is shown as a function of the scattering angle, at each of several laboratory energies, for single collisions of Ne^+ on Ne. The data can be regarded as showing at each energy the effect which variation of the internuclear distance of closest approach has upon the probability that the incident Ne^+ ion will capture an electron from the target Ne atom.

for the fraction of the scattered particles which are doubly ionized P_2, and Fig. 3 is the corresponding plot for the neutral fraction P_0 of the scattered particles. Empirical lines are drawn through the data points. Each data point represents the average of two or more data points obtained from independent runs, individual runs reproducing quite well the oscillations shown here.

The general trend with decreasing energy is for both P_1 and P_2 to decrease and for P_0 to grow correspondingly. No data for P_1 and P_2 are shown for energies below 3 keV since P_2 becomes less than a few percent at these energies and P_1 can be immediately inferred from P_0 since the sum of these two must now be approximately unity.

It should be observed that at the higher and lower energies shown in Fig. 3 the behavior of P_0 as a function of θ although qualitatively the same is quantitatively quite different. Thus, in the 6–15 keV energy range the peak-to-valley difference in P_0 is about 0.03, the average value of P_0 being near 0.10, while in the 0.8–1.3 keV energy range P_0 varies from a minimum of about 0.20 to about 0.65 for a maximum. In this connection it should be pointed out that the ordinate scale on the right side of Fig. 3 differs by a factor of 5 from that on the left side.

Figure 4 shows the data for a special experiment in which the heavy isotope of neon having mass number 22 was steered into the collision chamber. The focusing and magnetic analysis of the main beam were sufficiently good to provide essentially total resolution of Ne^{20} from Ne^{22} (the latter being about 9% abundant in naturally occurring neon), the former and more abundant isotope being used for all of the measurements of this paper except that shown in the upper part of Fig. 4. It is evident from the comparison of the Ne^{22} data with the Ne^{20} data shown in Fig. 4 that while the oscillations in P_1 and P_2 with θ are very much the same for the two cases, there is a shift in the angles at which the maxima and minima occur. The Ne^{22} experiment was undertaken especially to test the interpretation of the previously gathered data for Ne^{20}, and will be discussed further in the next section.

The following estimates are made for the accuracy of the data shown in Figs. 2–4. The laboratory angles for which the fractions P_0, P_1, and P_2 have their respective maxima and minima are considered to have been located to within $\pm 1/4$ deg. The maximum error generally ascribed to the magnitudes of these same fractions is $\pm 10\%$. However, for those cases where the fractions are changing rapidly with angle the error might be larger than this; the extreme angular width of acceptance of the detectors is $\pm 2/3$ deg, although most of the scattered particles come from a much narrower angular region about the chosen angle θ. At the lowest energies, where the SEM sensitivity for neutral particles becomes much less than that for singly ionized particles, there is an additional source of error in the determination of the selective sensitivity of the SEM as discussed in method (2) of the preceding section. The effect of this latter error would be to make all of the P_0 values at a given energy either too high or too low, while the effect of the $\pm 2/3$-deg angular reso-

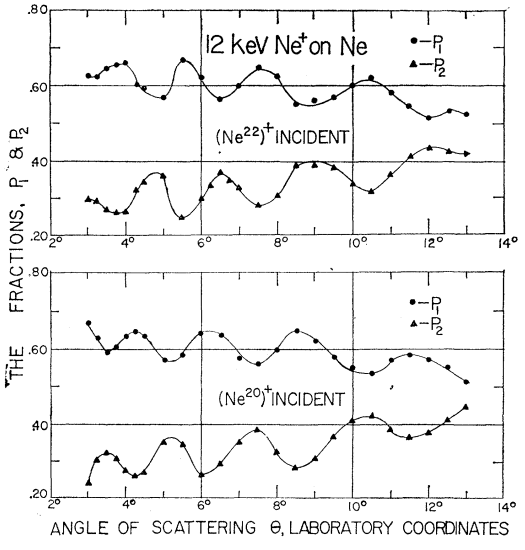

FIG. 4. The singly ionized and doubly ionized fractions of the scattered incident particles are shown vs scattering angle for two cases of 12-keV ions incident on Ne target atoms. The observed differences in the charge analysis for the two cases are attributed to the lesser speed, and consequently greater interaction time, for the heavier isotope.

lution is to lower the maxima and raise the minima. In particular then, some values of P_0 shown in the 0.8-keV data of Fig. 3 might be in error by as much as $\pm 20\%$.

5. INTERPRETATION OF DATA

In the Appendix to this paper it is shown that an application of Holstein's[4] description of resonant electron capture leads to the following expression for the electron capture probability P_0:

$$P_0 = A(v,r_0) + B(v,r_0)\sin^2 \times\left[(2\hbar v)^{-1}\int_{-\infty}^{+\infty}(E_r - E_a)ds\right], \quad (1)$$

where A and B are empirical functions of collision speed v and distance of closest approach r_0, and E_r and E_a are, respectively, the energies of the repulsive and attractive states of the $(Ne_2)^+$ molecular ion. The functions A and B are introduced to take account of the departure from pure resonance resulting from excitation and ionization during the collision.

With the proper choice of the functions A and B Eq. (1) gives a good fit to the data, A and B both being slowly varying monotonic functions of v and r_0 over most of the range of these two variables represented by the data. For sufficiently slow changes in A and B Eq. (1) tells us that the oscillations in P_0 should follow the oscillations in the sin term, the spacings of these oscillations together with the known values of v leading to an experimentally determined value for the integral which appears in that term.

Since the quantity $(E_r - E_a)$ is a function of internuclear separation, the integral in Eq. (1) is a function of the orbit of relative motion for the particular collision. However, for the relatively small scattering angles of this experiment it seems likely that this integral will be nearly the same along any two orbits for which the internuclear distance of closest approach r_0 is the same. Therefore we let

$$\int_{-\infty}^{+\infty}(E_r - E_a)ds = I(r_0), \quad (2)$$

where $I(r_0)$ is a function of r_0 only. Substituting Eq. (2) into Eq. (1) gives

$$P_0 = A(v,r_0) + B(v,r_0)\sin^2[I(r_0)/2\hbar v]. \quad (3)$$

Equation (3) now gives us a ready interpretation of the data shown in Fig. 3, where P_0 is shown to oscillate as a function of scattering angle θ for each of several fixed energies of incident ion; the oscillations in P_0 are caused by changing $I(r_0)$, increasing θ corresponding to decreasing r_0 and increasing $I(r_0)$, at fixed v.

An analysis was made of the experiment in which $(Ne^{22})^+$ was the incident particle to see if these data were consistent with the interpretation given to the rest of the data in which $(Ne^{20})^+$ was incident. The comparison of the data obtained for the two isotopes at an incident energy of 12 keV is shown in Fig. 4. The fractions P_1 and P_2 are shown vs θ in both cases since they show the oscillations more clearly than P_0, their oscillations being in phase and out of phase, respectively, with those of P_0. The curves for the heavier isotope are seen to be almost identical to those for the $(Ne^{20})^+$ except for being displaced to somewhat smaller angles. An analysis of these data via Eq. (3) shows that within experimental error the observed angular displacement is entirely accounted for by the lesser speed v of the heavier isotope; the difference in P_0 for the two isotopes at a particular scattering angle θ is a result of the increased interaction time for the heavier isotope.

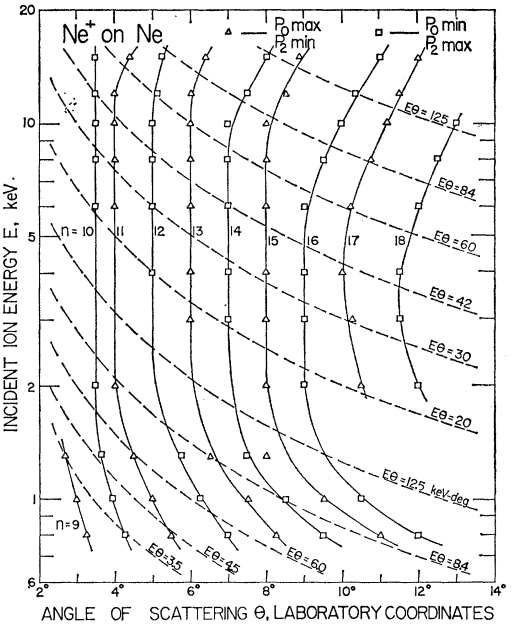

FIG. 5. The data of Fig. 3 were used to show here the various laboratory energies and angles for which the neutral fraction P_0 is a maximum or a minimum [i.e., $(\partial P_0/\partial\theta)_E = 0$] in single collisions of Ne^+ on Ne. For energies above 3 keV these maxima and minima of P_0 fall at the same scattering angles as do the minima and maxima of P_2 shown in Fig. 2. A solid line connects the points for each family of maximum P_0 or minimum P_0, an integer n being associated with each family. The dashed lines of constant $E\theta$ represent curves of constant internuclear distance of closest approach r_0, and play an important part in the interpretation of the data.

The resonant nature of the electron capture process would be even more evident if the data could be plotted to show P_0 vs $1/v$ at constant r_0 [hence $I(r_0) = \text{const}$]. According to Eq. (3) such a plot should show maxima and minima of P_0 occurring at regular intervals of $1/v$, the condition for an extremum in P_0 being

$$1/v = nh/2I, \qquad (n = 1,2,3,\cdots) \quad (4)$$

where odd n gives a maximum in P_0 and even n gives a minimum. If one conceives of a fixed interaction

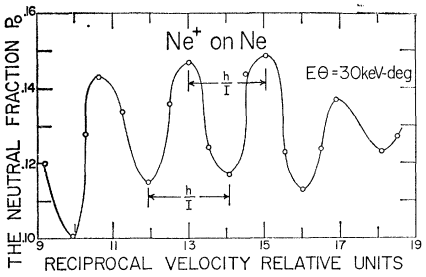

FIG. 6. The neutral fraction of the scattered incident particles is shown vs the reciprocal of the incident-ion velocity for collisions of constant $E\theta$. These are collisions of constant internuclear distance of closest approach r_0, the electron capture probability evidently varying from one extreme to the other as the collision time increases by approximately equal increments. For a given $E\theta$, and the corresponding r_0, the observed period of the resonance is related to the integral I as shown above and as explained in the text.

length for the collision then $1/v$ is proportional to the collision time, and these intervals would thus be proportional to the effective (average) period of the resonance. Figure 6 is such a plot showing just this behavior, and was obtained from the data through Fig. 5 in the following manner.

Figure 5 shows for each laboratory energy E of incident Ne^+ ion the laboratory angles θ at which the maxima and minima in P_0 were observed. (These maxima and minima always occurred at the same angles as the P_2 minima and maxima respectively whenever doubly ionized particles were a significant fraction of the scattered beam.) The solid lines are drawn through each family of maxima and minima, each family being characterized by an integer n, while the dashed lines are curves of approximately constant r_0 according to the small-angle approximation[12]

$$E\theta = F(r_0), \tag{5}$$

where $F(r_0)$ is a function of r_0 only. Each point appearing on Fig. 6, in which P_0 is plotted vs $1/v$, was obtained from a point on the $E\theta = 30$ keV-deg curve of Fig. 5 by using the collision speed v corresponding to the laboratory collision energy E, and determining P_0 for the particular values of E and θ by use of the data of Fig. 3.

It is evident from Eq. (4) that the intervals between adjacent maxima (and adjacent minima) in Fig. 6 should all have the value

$$\Delta(1/v) = h/I, \tag{6}$$

and that I can then be determined from the measured speeds v. This has been done for the data of Fig. 6 and the relative units of reciprocal velocity shown in that figure were then chosen so that $h/2I = 1$, making $1/v$ numerically equal to n. With this choice of units it then appears that the values of the integers n characterizing the maxima and minima of Fig. 6, and also the corresponding families of maxima and minima of Fig. 5, are $n = 10$ through $n = 18$. Once this assignment of n values has been made I may also be determined from Eq. (4) as

$$\int_{-\infty}^{+\infty} (E_r - E_a)ds \equiv I = nvh/2. \tag{7}$$

Although the calculation of I from Eq. (7) is in principle quite equivalent to that from Eq. (6), there appears to be some improvement in accuracy when using the data in Eq. (7).

Figure 7 shows I, which is the quantity $(E_r - E_a)$ integrated over the path of relative motion, vs the product $E\theta$ in laboratory coordinates. For each value of $E\theta$ the integral I has been calculated from the data via Eq. (7) for as many pairs of n and v as there are intersections of that $E\theta$ curve with the data lines on Fig. 5. For $E\theta$ values from 125 keV-deg to 12.5 keV-deg inclusive, this amounted to from 7 to 9 independent calculations for each $E\theta$, all of which were within 2% of the mean value shown as the ordinate of Fig. 7. The fact that such close agreement was achieved is considered strong evidence for the basic validity of our interpretation of the data.

It would seem desirable to know I as a function of the distance of closest approach r_0. However, the functional dependence of $E\theta$ upon r_0 depends upon the potential energy function for the $Ne^+ - Ne$ system over the range of internuclear separations from about 0.2 to 1.0 Å and there is still some uncertainty about this latter function. Consequently, Fig. 8 shows the functional dependence of $E\theta$ upon r_0 as determined from each of two exponentially screened Coulomb potential energy functions.

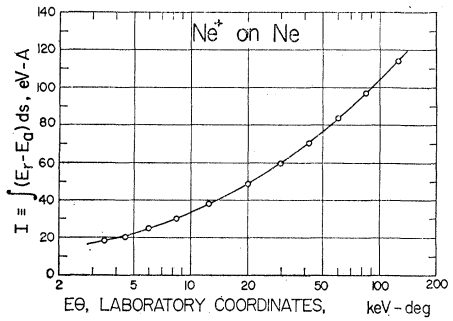

FIG. 7. The data of this experiment are interpreted as giving the functional dependence of the integral I upon the product $E\theta$ (which here has the same value in laboratory and center-of-mass coordinates), the latter depending in turn on the internuclear distance of closest approach r_0. The E_r and E_a of the integrand are, respectively, the energies of the repulsive and attractive states of the $(Ne_2)^+$ molecular ion, the integration being performed over the collision path of relative motion.

[12] This approximation can be obtained from Eq. (17) of reference 5, which implies that the product $E\theta$ is a function only of r_0 for small-angle scattering by an exponentially screened Coulomb potential. Also, considerations of a more general nature show that this should be a good approximation for small-angle scattering by any repulsive central force which falls off rapidly with increasing distance. Note that $E\theta$ has the same value in laboratory and center-of-mass coordinates for the collision of an incident particle with a target of equal mass.

The upper curve was obtained using the potential energy function suggested by Bohr,[13] and the lower curve was obtained using the exponentially screened Coulomb potential energy function which best fits the experimentally determined function of Lane and Everhart.[6] This latter function was determined from measured differential scattering cross sections for collisions at 25 keV and extends from internuclear separations of about 0.10 to 0.16 Å, appearing everywhere in this region to be about 0.6 of Bohr's function. The lower curve of Fig. 8 was obtained in effect then by extrapolating the empirical potential energy function of Lane and Everhart into the region from about 0.2 to 1.0 Å. Both of the curves in Fig. 8 were computed from the respective potentials using the calculations of Everhart *et al.*[5] It is the opinion of the present authors that the curve obtained from the potential energy function of Lane and Everhart is the more reliable of the two.

If one uses this lower curve of Fig. 8 together with the data of Fig. 7 he can obtain the integral I as a function of r_0, from which he can then determine something about the functional dependence of (E_r-E_a) upon internuclear separation R. This was done by assuming that (E_r-E_a) is an exponentially decreasing function[14] of R and performing the integration over a straight line path which is tangent to the actual collision path at the point of minimum internuclear separation. It was found that the values of I so obtained agree with the measured values of I to within 3% when

$$(E_r-E_a)=(390\text{ eV})\exp(-R/0.22\text{ Å}),\quad (0.2\text{ Å}<R<0.8\text{ Å}). \quad (8)$$

It is difficult to assign limits of error to Eq. (8) since its accuracy is contingent upon not only the accuracy of our data and the validity of our rather simple interpretation but also the accuracy of the transformation from $E\theta$ to r_0. However, error introduced by the first of these three sources should amount to less than 10%.

A concluding observation is that a critical value of r_0 appears to separate those collisions characterized by simple resonant electron exchange from those (of smaller r_0) for which this resonance plays only a small role in the electron capture probability. Figure 3 shows this separation to occur in the vicinity of $E\theta=12$ keV-deg which, according to the lower curve of Fig. 8, corresponds to $r_0=0.5$ Å. This critical value of the internuclear distance of closest approach can be compared to 0.32 Å for the radius of maximum radial charge density of the $2p$ electrons in neon, the relative magnitudes of these numbers giving some idea about the overlap of the two atomic systems which accompanies the transition from one type of collision to the other.

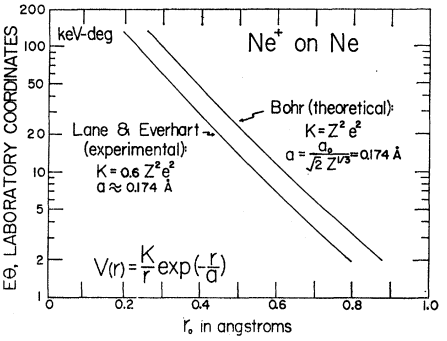

FIG. 8. The relationship between the product $E\theta$ and the internuclear distance of closest approach r_0 is shown for each of two exponentially screened Coulomb potential energy functions. The measurements of this paper yield no information about the functional dependence of $E\theta$ upon r_0, and this graph is included so that the reader can transform the observed values of $E\theta$ shown in Fig. 7 into the corresponding values of r_0. In this way the data of this experiment can be interpreted as giving the functional dependence of the integral I upon r_0.

ACKNOWLEDGMENTS

The authors wish to express their thanks to Mark F. Taylor and David C. Morrison for the many calculations they performed in analyzing the data of this experiment. Special thanks are also due Modest Poudrier for the skillful machining of the numerous mechanical components of the apparatus. Finally, we are indebted to Dr. Edgar Everhart for several valuable suggestions resulting from his reading of a preliminary version of this manuscript.

APPENDIX. RESONANT ELECTRON CAPTURE

In dealing with ion-atom collisions within the range of kinetic energies and scattering angles of this experiment, one is justified in using a classical trajectory (impact parameter method) for the scattering event since the deBroglie wavelength of the incident particle is much less than the impact parameter of the collision. In this experiment the de Broglie wavelength of the incident Ne^+ is of the order of 10^{-3} Å while the impact parameter is always greater than 10^{-1} Å. Furthermore, the collision is moderately slow when compared with the motion of the electrons in the outer orbits of the atom. Here the speed of the incident Ne^+ varied from about 0.03 to 0.1 that of the electrons in the outer orbits of neon. Thus, it would seem appropriate to describe the collision in terms of the electronic wave functions of the $(Ne_2)^+$ molecular ion and the adiabatic approximation of time-dependent perturbation theory.

This kind of description of the interaction of a positive ion with a neutral atom of the same species has

[13] N. Bohr, Kgl. Danske Videnskab, Selskab, Mat.-fys. Medd. 18, 8 (1948).

[14] This same functional dependence was assumed by F. P. Ziemba in his Doctoral thesis, University of Connecticut, 1960 (unpublished). His interpretation of the Ne^+ on Ne data of reference 3 is based upon an equation derived in reference 8 which is equivalent to Eq. (A2) of this paper, and leads him to an estimate of (E_r-E_a) as a function of R. His function gives values about 25% higher than those obtained from Eq. (8) above, which we consider good agreement in view of the limited range of data available to him.

been given by Holstein[4] in a consideration of the mobility of a positive ion in its parent gas. (The recent book edited by Bates[11] contains a very similar treatment of this same problem.) In particular, he is concerned with the capture of an electron from the neutral target atom by the incident positive ion. The wave function he uses is a linear superposition of the energy eigenfunctions for the attractive and repulsive states of the diatomic, homonuclear, molecular ion. The space part of the attractive state is the familiar symmetric combination of the ground state, unperturbed, atomic states ϕ_A and ϕ_B which correspond, respectively, to the electron being with atom A, the target, and with atom B, the incident system. Similarly, the space part of the repulsive state is the antisymmetric combination of ϕ_A and ϕ_B. The time-dependent perturbation takes the form of making both of these space states actually functions of time via the time-changing internuclear separation, and also replaces the phases $E_r t/\hbar$ and $E_a t/\hbar$ of the stationary-state functions by the corresponding time-integrated values, since the energies E_r and E_a (of the repulsive and attractive states respectively) are now time dependent. A few algebraic manipulations then lead to an expression for the time-dependent wave function for the system in the form

$$\psi(t)=[a(t)\phi_A+b(t)\phi_B]\times\exp\left[-i\int_{t_i}^{t}(E_r+E_a)dt/2\hbar\right], \quad \text{(A1)}$$

where t_i is the time at the start of the interaction. The square of $b(t)$ represents the probability of the electron being found with the incident ion at time t, and if t is chosen to be a time t_f after the interaction has terminated then b^2 represents the probability P_0 that the electron has been captured as a result of the encounter. Thus Holstein's result is

$$P_0=b^2(t_f)=\sin^2\left[\int_{-\infty}^{+\infty}(E_r-E_a)dt/2\hbar\right], \quad \text{(A2)}$$

there being no difficulty associated with letting $t_i\rightarrow-\infty$ and $t_f\rightarrow+\infty$.

The description given by Holstein is then one of resonant electron capture where an electron initially with the target atom alternates back and forth between the two atomic systems with a variable frequency $(E_r-E_a)/h$ during the course of the collision. We have an exact resonance inasmuch as the electron has the same energy in the two degenerate states ϕ_A and ϕ_B.

It is evident that this description is less applicable to the collisions of the present paper than to the less energetic ones in a typical ion mobility experiment, there being no provision in the description for excitation and ionization of the colliding systems. Nevertheless, it seems profitable to apply this description under the following assumption: For these energetic collisions, the conditions for maximum and minimum probability of electron capture are precisely those given by Holstein's result, the effect of excitation and ionization being merely to reduce the amplitude of oscillation and mean value of P_0 from that predicted by Eq. (A2). We may express this assumption by writing that P_0 should be given by

$$P_0=A(v,r_0)+B(v,r_0)\sin^2\left[\int_{-\infty}^{+\infty}(E_r-E_a)dt/2\hbar\right], \quad \text{(A3)}$$

where both $A(v,r_0)$ and $B(v,r_0)$ are slowly varying, monotonic functions of the collision speed v and internuclear distance of closest approach r_0.

In applying this description to the present situation it is advantageous to replace dt by ds/v in Eq. (A3) and perform the integration over the path of relative motion. Furthermore, for the moderately small angles of scattering studied, the relative speed v remains nearly constant during the collision, so that to a good approximation the electron capture probability P_0 becomes

$$P_0=A(v,r_0)+B(v,r_0)\sin^2\times\left[(2\hbar v)^{-1}\int_{-\infty}^{+\infty}(E_r-E_a)ds\right]. \quad \text{(A4)}$$